ADVANCED MATERIALS

# Supporting Information

for *Adv. Mater.,* DOI: 10.1002/adma.202101500

# Hydrophilicity-Hydrophobicity Transformation, Thermoresponsive Morphomechanics, and Crack Multifurcation Revealed by AIEgens in Mechanically Strong Hydrogels

*Yubing Hu, Lucile Barbier, Zhao Li, Xiaofan Ji, Heiva Le Blay, Dominique Hourdet, Nicolas Sanson, Jacky W. Y. Lam,* Alba Marcellan,* and Ben Zhong Tang**

**Materials and instrumentation**

All the chemicals were reagent grade and used as received without further purification. 4-Bromo-*N*,*N*-diphenylaniline, 4-vinylpyridine, 2-bromoethanol, acryloyl chloride, palladium(II) acetate, tri(*o*-tolyl)phosphine, sodium sulfate, *N*-isopropylacrylamide (NIPAM), *N*,*N*-dimethylacrylamide (DMA), *N*,*N*′-methylenebisacrylamide (MBA), potassium peroxodisulfate (KPS), *N*,*N*,*N*′,*N*′-tetramethylethylenediamine (TEMED), 2-aminoethanethiol hydrochloride, acetic acid, sodium hydroxide (NaOH), acrylic acid and *N*,*N*′-dicyclohexylcarbodiimide (DCCI) were purchased from Sigma-Aldrich and J&K Scientific. Polybutadiene (PB, $M_w$ = 200,000 g/mol), polystyrene (PS, $M_w$ = 280,000 g/mol), poly(methyl methacrylate) (PMMA, $M_w$ = 120,000 g/mol) and poly(ethylene glycol) (PEG, $M_w$ = 20,000 g/mol) were purchased from Sigma-Aldrich for the preparation of polymer thin films. Chitosan (85% deacetylated), PEG ($M_w$ = 6,000 g/mol), α-cyclodextrin, Pluronic® F-127 (PEG-PPG-PEG, $M_w$ = 12,600 g/mol) and Mowiol® PVA-117 (Poly(vinyl alcohol), $M_w$ = 145,000 g/mol) were purchased from Sigma-Aldrich and Meryer for the preparation of stimuli-responsive hydrogels. All the organic solvents including toluene, acetone, dimethyl sulfoxide (DMSO) and methanol (MeOH), triethylamine, dichloromethane (DCM), hexane, ethyl acetate, triethylamine (TEA), dimethylformamide (DMF), *N*-methyl-2-pyrrolidone (NMP), deuterated dimethyl sulfoxide (DMSO-$d_6$) and deuterated chloroform ($CDCl_3$) were purchased from Sigma-Aldrich. Nitrogen came from the fume hood through the center gas lines in Department of Chemistry, the Hong Kong University of Science and Technology. Water was purified with a Millipore system with inverse osmosis membrane (Milli RO) and ion exchange resins (Milli Q).

$^1H$ and $^{13}C$ NMR spectra were obtained on a Bruker ARX 400 NMR spectrometer in DMSO-$d_6$ and $CDCl_3$ with tetramethylsilane (TMS; $\delta$ = 0 ppm) as internal reference. High-resolution mass spectra (HRMS) were recorded on a GCT premier CAB048 mass spectrometer operating in MALDI−TOF mode. Gel permeation chromatography (GPC) was performed in water at an elution rate of 1.0 mL/min on a Waters Associates GPC system equipped with a Waters 1515 HPLC pump

and interferometric refractometer detector. Standard poly(methyl methacrylate)s were utilized for plotting calibration curves to determine the number-average molecular weights ($M_n$) and the weight-average molecular weight ($M_w$). The polymer samples (2 mg/mL) dissolved in sodium hydroxide solutions (0.02 M) were filtered through a 0.45 μm PTFE filter and then injected into the GPC system. Ultraviolet–visible (UV-vis) absorption spectra were collected on a Hewlett-Packard 8453 spectrophotometer equipped with a temperature controller (± 0.1 °C). Transmittance curves were built by collecting the absorbance at 600 nm with a scanning rate of 0.3 °C/min. Photoluminescence (PL) spectra were measured on a Horiba Fluorolog spectrophotometer. Fluorescence quantum yields were measured using a Horiba Quanta-φ accessory combined with a Horiba fluorometer. Fluorescent images were taken on a ZEISS Axio Vert.A1 FL fluorescent microscope with Axiocam 305 color camera through a ZEN lite microscope software under ultraviolet light excitation (330-385 nm). The viscoelastic properties of the hydrogels were studied using a stress-controlled rheometer (DHR3 from TA Instruments) equipped with a roughened plate/plate geometry (diameter 20 mm, gap of 2 mm) and a temperature controller (Peltier). Tensile tests were performed on a standard tensile Instron machine model 5565, equipped with a 10 N load cell (with a relative uncertainty of 0.16% in the range from 0 to 0.1 N) and an environmental chamber with a temperature controller. Temperature-dependent Infrared spectra were collected on a Thermo Scientific Nicolet iS50 FTIR Spectrometer equipped with Specac® Golden Gate Single Reflection Diamond ATR.

**Synthesis and characterization.**

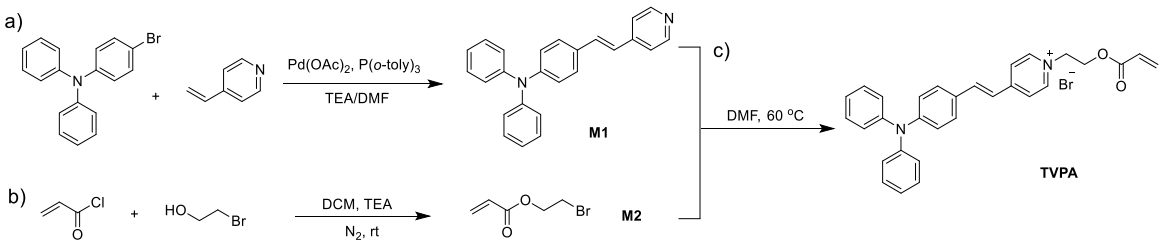


**Figure S1**. Three-step synthetic routes to **TVPA**.

**Synthesis of M1**: A typical procedure for Heck cross-coupling reaction was conducted to synthesis **M1** from the starting materials of 4-bromo-*N*,*N*-diphenylaniline (2.53 g, 7.8 mmol) and 4-vinylpyridine (1.07 g, 1.02 mmol). The crude product was purified by column chromatography ($SiO_2$; DCM/hexane, v/v = 1:1). Yellow solid (1.67 g, 59% yield). $^1$H NMR ($CDCl_3$, 400 MHz): δ (ppm) = 6.90–6.94 (d, J = 16 Hz, 1H), 7.08–7.12 (t, J = 8 Hz, 4H), 7.15–7.17 (d, J = 8 Hz, 4H), 7.30–7.33 (m, J = 12 Hz, 7H), 7.36–7.37 (d, J = 4 Hz, 2H), 8.57–8.58 (d, J = 4 Hz, 2H). $^{13}$C NMR ($CDCl_3$, 100 MHz): $\delta$ (ppm) = 120.67, 122.85, 123.54, 124.93, 128.02, 129.44, 129.83, 132.70, 144.99, 147.30, 148.47, 150.17. HRMS (MALDI-TOF): *m*/*z*: $[M]^+$ calcd for $C_{25}H_{20}N_2$, 348.1626; found, 348.1750.

**Synthesis of M2**. **M2** was synthesized according to a previously reported procedure.[1] 2-Bromoethanol (1.24 g, 10 mmol) was added into a two-necked flask, and then the flask was evacuated and refilled with nitrogen three times. DCM (30 mL) was added and the solution was cooled down in an ice bath. Triethylamine (1.4 mL) was injected at 0 °C. Acryloyl chloride (0.90 g, 10 mmol) dissolved in DCM (2 mL) was added dropwise. The reaction mixture stirred overnight after warming to room temperature. Upon completion, the reaction mixture was filtered, the solid residue was washed with DCM and the organic layer was washed with water three times. The organic layer was dried over anhydrous $Na_2SO_4$ and the organic solvent was removed by rotary evaporation under reduced pressure to get the product (1.52 g, 85% yield, colorless liquid). $^1$H NMR (CDCl3, 400 MHz): 3.49–3.53 (t, J = 8 Hz, 2H), 4.41–4.44 (t, J = 6 Hz, 2 H), 5.83–5.85 (d, J = 8 Hz, 1 H), 6.10–6.14 (dd, J = 8, 4 Hz, 1 H), 6.40–6.44 (d, J = 16 Hz, 1 H). $^{13}$C NMR ($CDCl_3$): $\delta$ = 63.82, 127.81, 128.59, 31.65, 165.52.

**Synthesis of TVPA. M1** (1.45 g, 4 mmol) and **M2** (0.86g, 4.8 mmol) were dissolved in DMF and the reaction mixture was stirred at 80 °C overnight. Upon completion indicated by a thin layer chromatography (TLC) plate, the reaction mixture was filtered, the solid residue was washed with

DCM and the organic layer was washed with water three times. The organic layer was dried over anhydrous $Na_2SO_4$ and the organic solvent was removed by rotary evaporation under reduced pressure. The crude product was purified by column chromatography ($SiO_2$; DCM/ethyl acetate, v/v = 1:1). Red solid (1.45 g, 69 % yield). $^1$H NMR (DMSO-$d_6$, 400 MHz): δ (ppm) =4.60–4.62 (t, J = 4 Hz, 2H), 4.80–4.82 (t, J = 4 Hz, 2H), 5.97–6.00 (d, J = 12 Hz, 1 H), 6.10–6.17 (d, J = 8 Hz, 1 H), 6.30–6.34 (d, J = 16 Hz, 1H), 6.93–6.95 (d, J = 8 Hz, 2H), 7.11–7.13 (d, J = 8 Hz, 4 H), 7.16–7.18 (t, J = 4 Hz, 2H), 7.36–7.40 (m, J = 8 Hz, 5H), 7.62–7.64 (d, J = 8 Hz, 2H), 7.97–8.01 (d, J = 16 Hz, 1 H), 8.15–8.19 (t, J = 8 Hz, 2 H), 8.89–8.91 (d, J = 8 Hz, 2H). $^{13}$C NMR (DMSO-$d_6$, 100 MHz): $\delta$ (ppm) = 58.05, 62.63, 120.34, 120.49, 120.58, 122.90, 123.01, 124.37, 125.25, 127.46, 127.91, 129.71, 129.75, 132.38, 141.16, 146.06, 149.45, 153.74, 164.73. HRMS (MALDI-TOF): *m*/*z*: $[M+H]^+$ calcd for $C_{30}H_{28}BrN_2O_2$, 527.1336; found, 527.1318.

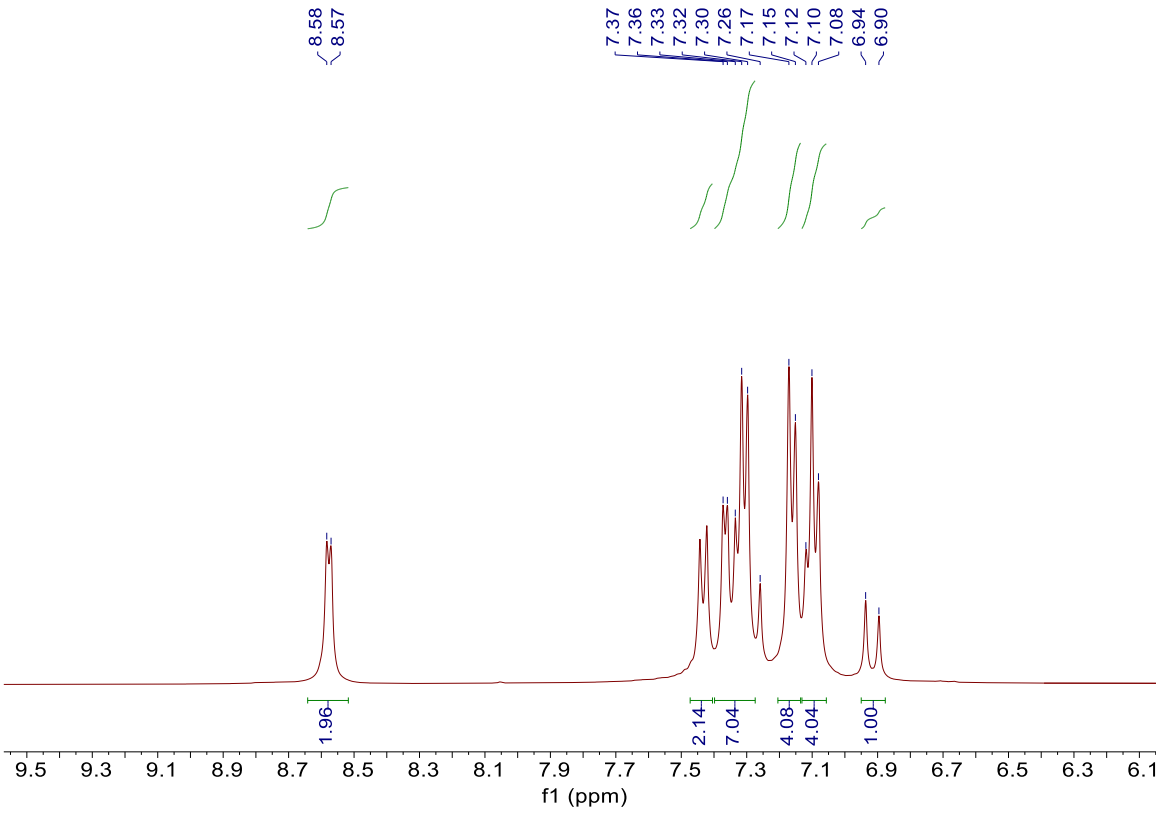


**Figure S2**. $^1$H NMR spectrum of **M1** in $CDCl_3$.

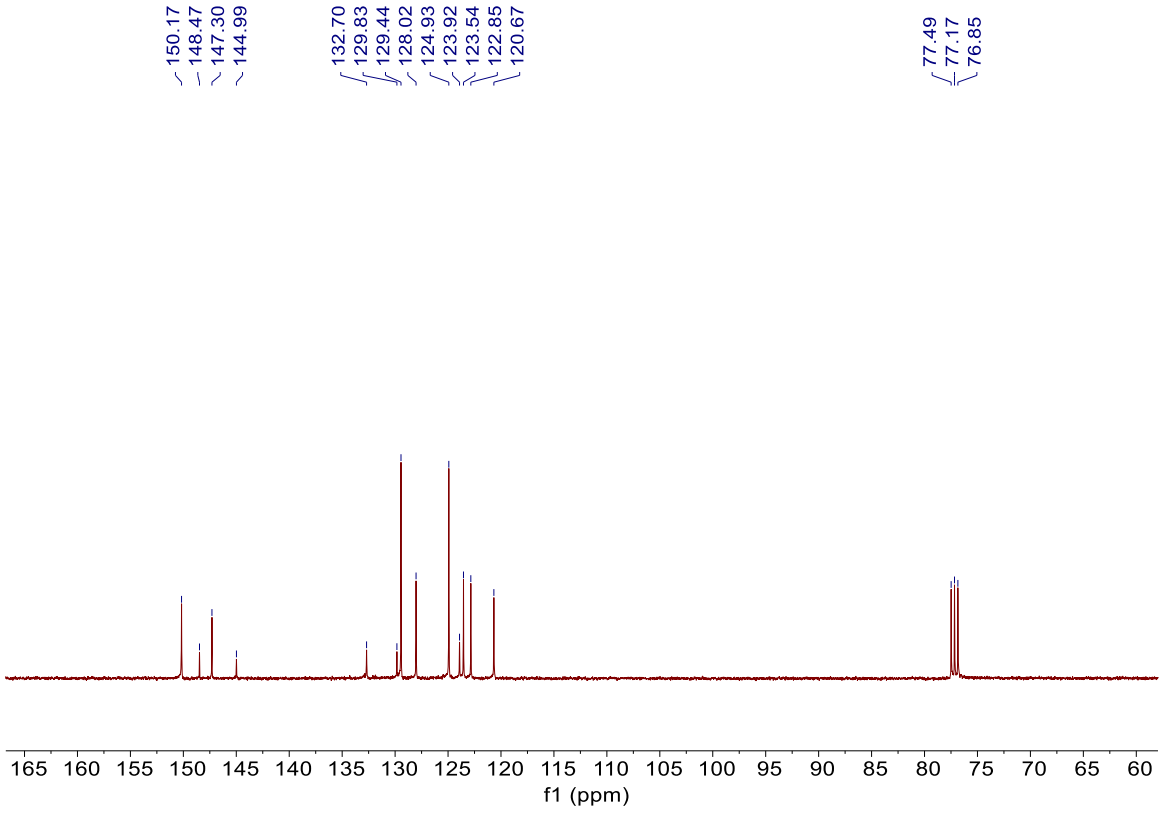


**Figure S3**. $^{13}C$ NMR spectrum of **M1** in $CDCl_3$.


**Figure S4**. Mass spectrum of **M1**.

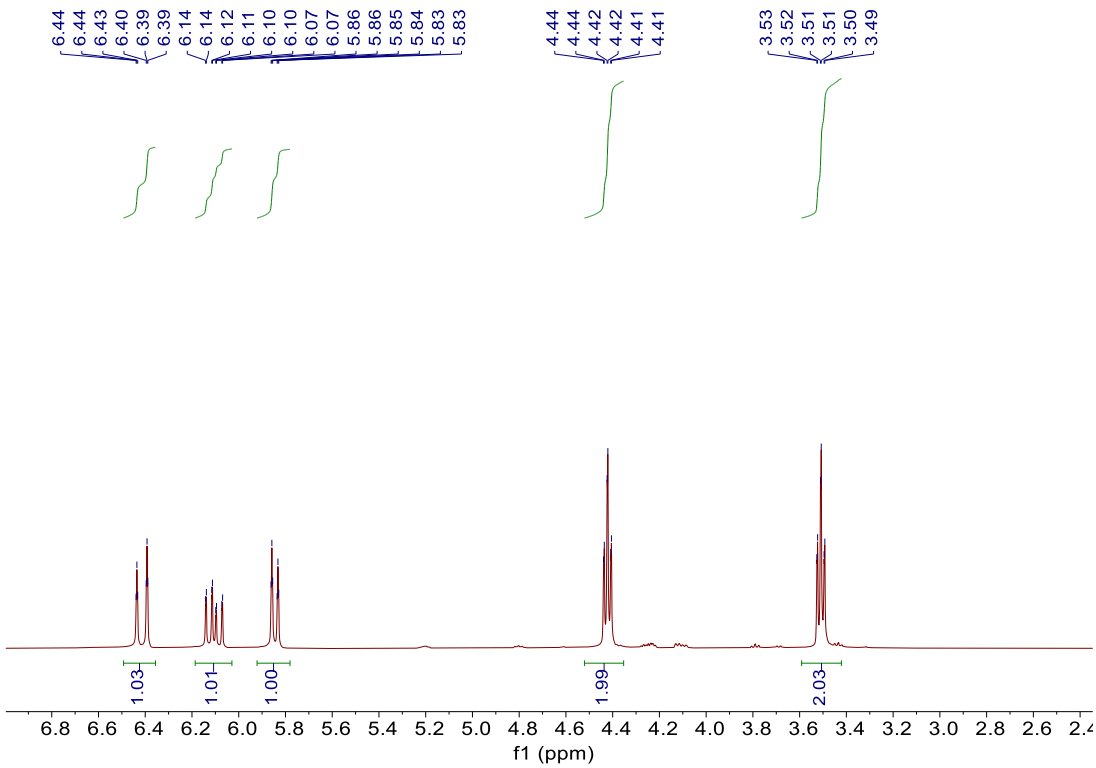


**Figure S5**. $^{1}$H NMR spectrum of **M2** in $CDCl_3$.

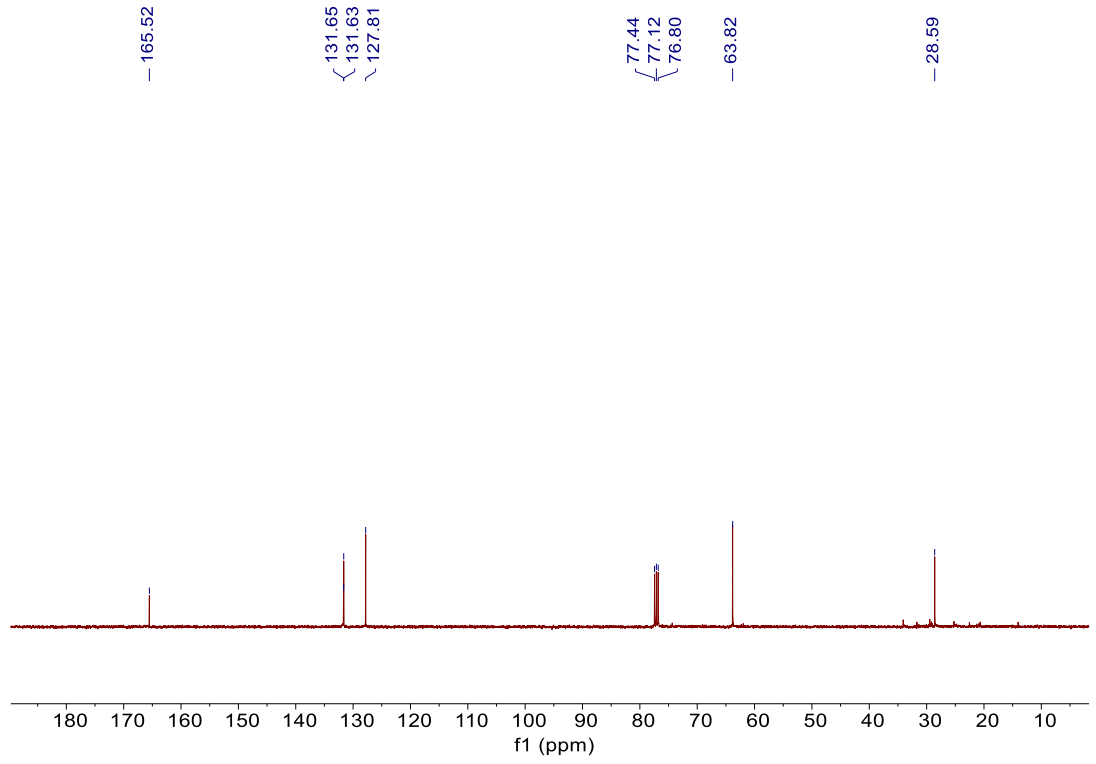


**Figure S6**. $^{13}$C NMR spectrum of **M2** in $CDCl_3$.

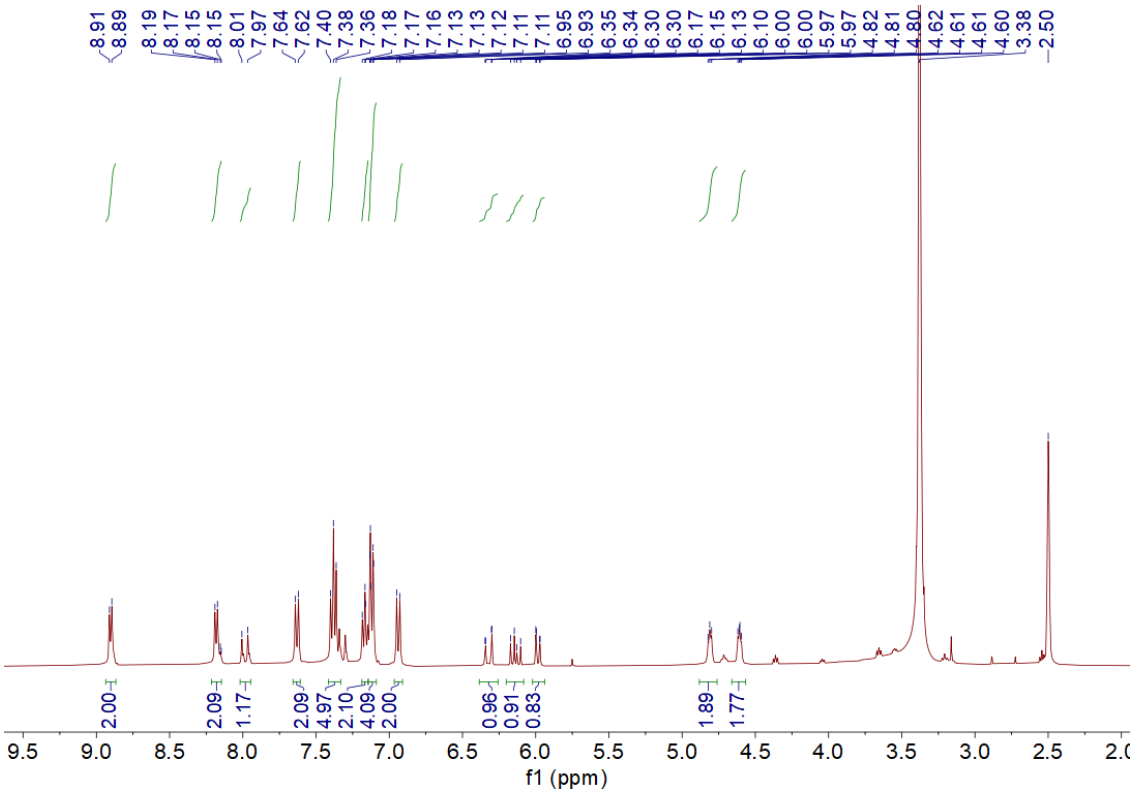


**Figure S7**. $^{1}$H NMR spectrum of **TVPA** in DMSO-$d_6$.

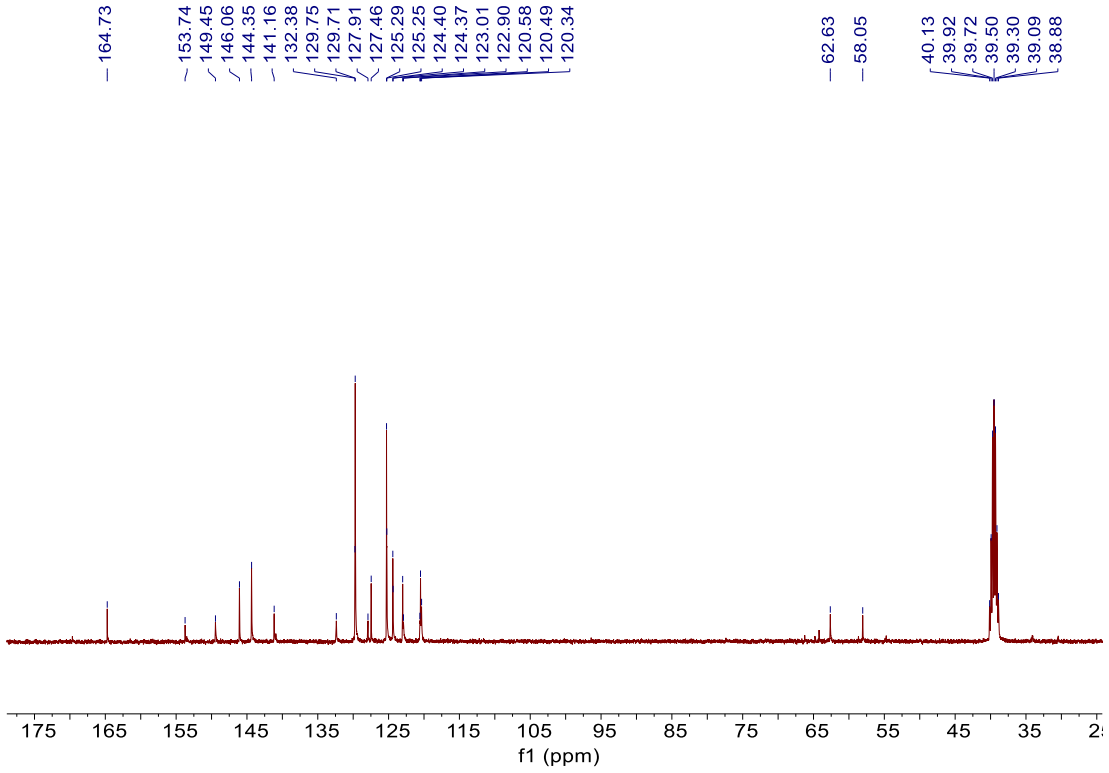


**Figure S8**. $^{13}$C NMR spectrum of **TVPA** in DMSO-$d_6$.

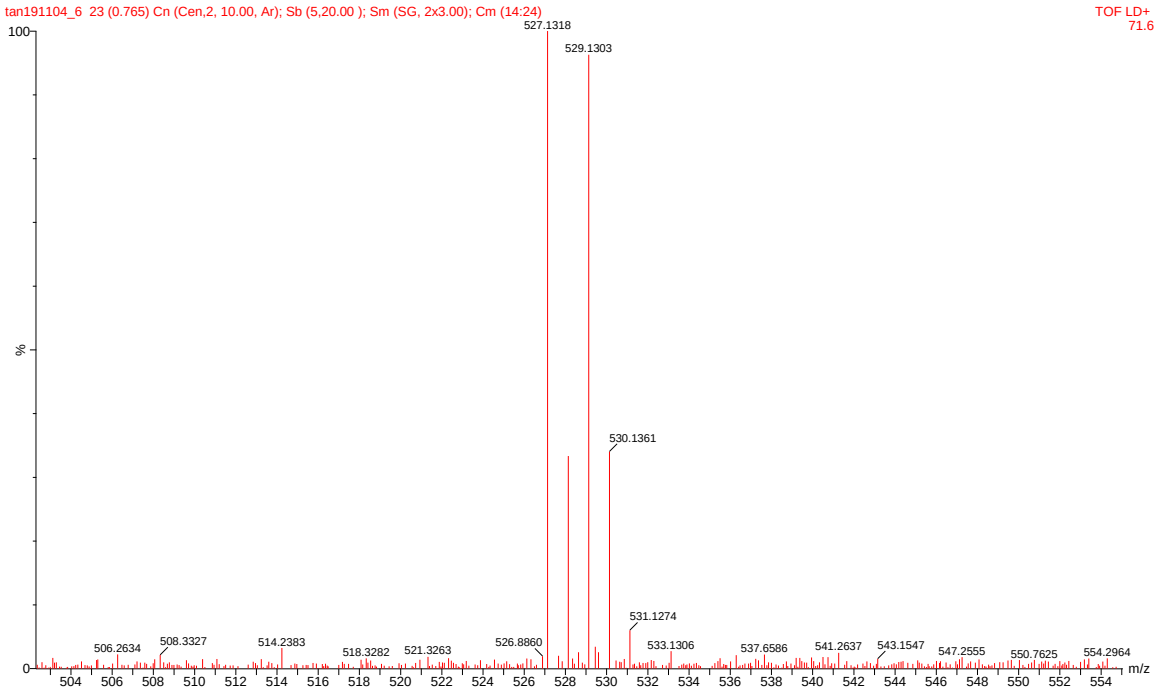


**Figure S9**. Mass spectrum of **TVPA**.

## Synthesis of PDMA macromonomers

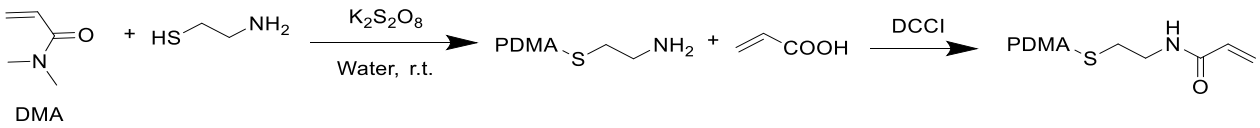


**Figure S10**. Synthetic route to PDMA macromonomer.

**Synthesis of Amino-Terminated Telomers**. Functional polymer chains were prepared by free radical polymerizations using 2-aminoethanethiol hydrochloride (AET·HCl) as chain transfer agent. In a two-necked flask, 0.2 mol of DMA monomers was dissolved in 500 mL of water and the mixture was deoxygenated by nitrogen bubbling for 1 h. The redox initiators, KPS (4.6 mmol) and AET·HCl (3.1 mmol), were separately dissolved in 10 mL of water and deoxygenated for 30 min before adding into the reaction medium. The reaction mixture was stirred overnight in an ice bath. 2 mL of NaOH solutions (2 M) were added to neutralize the ammonium end-group and the polymer solution was freeze-dried (10.8 g).

**Synthesis of PDMA macromonomers.** 10 g of amino-terminated PDMA chains and acrylic acid (2.23 g, 31 mmol) were dissolved in 100 mL of NMP. DCCI (3.19 g, 155 mmol) was dissolved in 5 mL of NMP and then injected into the reaction mixture. The reaction was stirred overnight at room temperature. After dilution with 200 mL of water, the polymer was purified by dialysis against pure water (membrane cut-off = 12 kDa) for one week. Finally, the polymer solution was filtered and the filtrate was freeze dried to obtain PDMA macromonomers (9.6 g, $M_n$ = 240,000 g/mol, $M_w/M_n$ = 1.6).

**Preparation of hydrogels**

Monomers (NIPAM, TVPA and PDMA macromonomers), crosslinker (stock solution of MBA) and initiator (stock solution of KPS) were initially dissolved in water. The reaction mixture was degassed by nitrogen bubbling in an ice bath for 30 min. Then all the solutions were mixed and TEMED was added into the reaction medium at room temperature under a nitrogen atmosphere. After fast mixing (30 s), the precursor solution was rapidly transferred between glass plates of 2 mm width, and the reaction was left to proceed overnight at room temperature to get the as-prepared hydrogels (the hydrogels at the preparation state). The same molar ratio of crosslinker and initiator to NIPAM monomer in all hydrogels were controlled to keep the constant density of elastically active chains.

**Table S1.** Formulation of hydrogels[a]

| Gel | NIPAM (wt%) | PDMA (wt%) | PDMA/N (%) | TVPA/N (%) | MBA/N (%) | KPS/N (%) | TEMED/N (%) | $Q_a$[b] |
|---|---|---|---|---|---|---|---|---|
| GN2D3 | 8.30 | 12.45 | 0.071 | 0.5 | 0.2 | 0.3 | 0.3 | 4.8 |
| GN3D3 | 8.30 | 8.30 | 0.047 | 0.5 | 0.2 | 0.3 | 0.3 | 6.0 |
| GN6D3 | 8.30 | 4.15 | 0.024 | 0.5 | 0.2 | 0.3 | 0.3 | 8.0 |
| GN | 8.30 | / | / | 0.5 | 0.2 | 0.3 | 0.3 | 11 |
| GD[c] | / | 8.30 | 0.047 | 0.5 | 0.2 | 0.3 | 0.3 | 11 |

[a]NIPAM (wt%) refers to the weight ratio of NIPAM to the precursor solution. PDMA/N, TVPA/N, MBA/N, KPS/N and TEMED/N refers to the molar ratio of PDMA, TVPA, MBA, KPS and TEMED to NIPAM,

respectively. [b]$Q_a$ refers to the swelling degree of the as-prepared hydrogels. [b]GD was prepared from 8.30 wt% *N*,*N*-dimethylacrylamide.

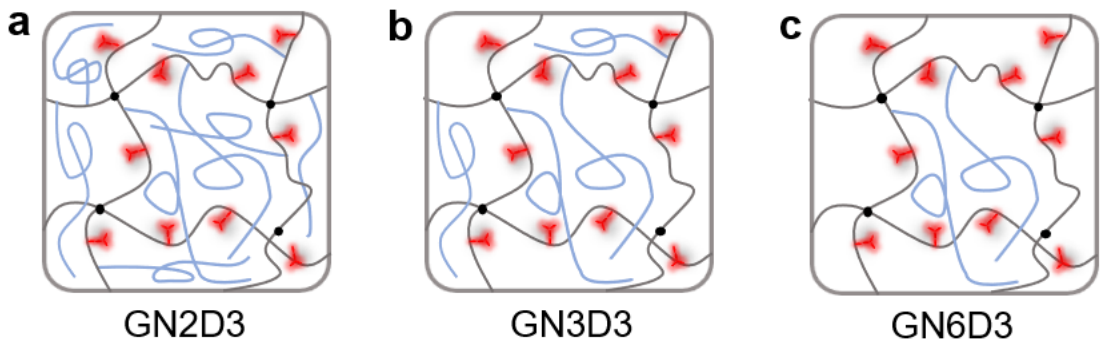


**Figure S11.** Gel topologies for the as-prepared hydrogels.

**Preparation of hydrogels with stimuli-responsive gelation**

Aqueous solution of chitosan (0.02 g/mL) was prepared by dissolving TVPA and chitosan in water and its pH was tuned to 5.6 by adding acetic acid. The NaOH solution (0.01 M) was poured slowly into the chitosan solution. The gelation of chitosan was induced by the diffusion of NaOH.[2]

Aqueous solutions of PEG (0.013 g/mL) and α-CD (0.145 g/mL) were prepared by dissolving PEG and α-CD with TVPA in water at 50 °C, respectively. The equal volume of PEG and α-CD solutions was mixed at 50 °C and the mixture was gelled after standing at 20 °C for 24 h.[3]

Aqueous solution of PEG-PPG-PEG (18 wt%) was prepared by dissolving TVPA and PEG-PPG-PEG in water at 90 °C and cooled down at room temperature. The fluorescent photos of PEG-PPG-PEG solutions at 5 °C were collected after cooling in a refrigerator. The PEG-PPG-PEG solution was gelled along the glass inner wall by stirring the glass vials slowly in the temperature-controlled oven.[4]

**Swelling measurement**

Equilibrium swelling experiments of hydrogels were performed in water at designated temperatures. For each hydrogel of different composition, three hydrogel samples were cut into the same size and placed in a large excess of water for one week to obtain the average weight of the

swollen hydrogel ($m_e$). The swollen hydrogel samples were dried in an oven at 50 °C for two days to obtain the average weight of the dry hydrogel ($m_d$). The swelling degree ($Q$) of hydrogels can be calculated as $Q = m_e/m_d$.

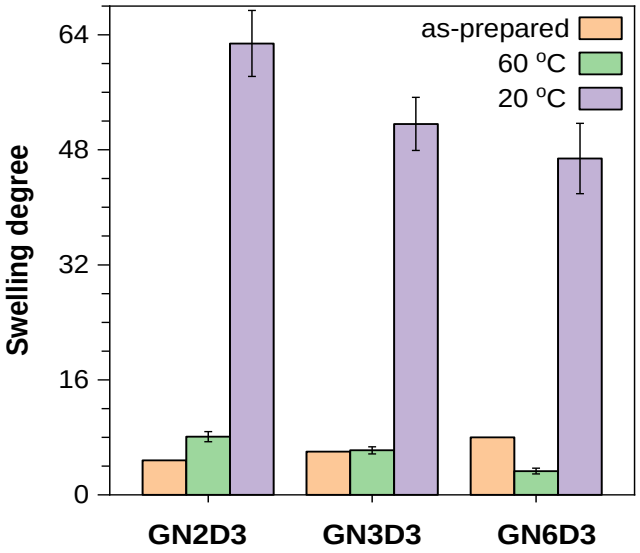


**Figure S12**. The swelling degree of hydrogels in the as-prepared state, the thermodynamic equilibrium at 20 °C and 60 °C in water.

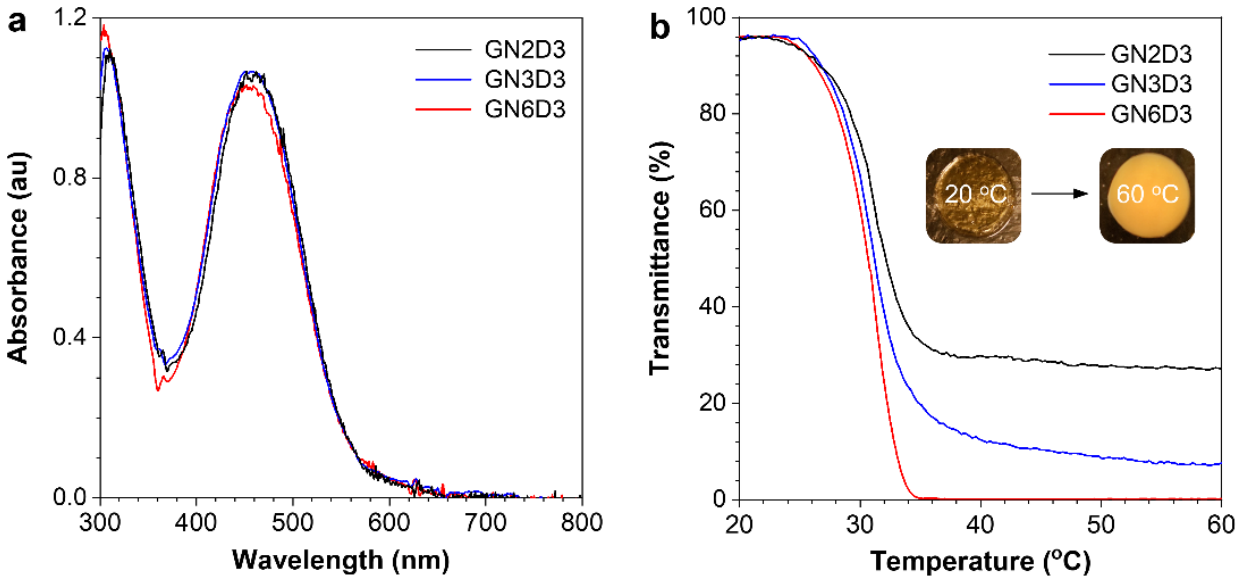

**Figure S13**. **a**, UV-vis spectra of the as-prepared GN2D3, GN3D3 and GN6D3 at 20 °C. **b**, Temperature-dependent transmittance of GN2D3, GN3D3 and GN6D3 from 20 °C to 60°C at a heating rate of 0.3 °C/min determined by the absorption intensity at 600 nm.

**Morphological observation by fluorescence microscope**

The hydrogel samples were immersed in water at designated temperatures for 30 min and then were placed in the glass slides at room temperature before the morphological observations using an inverted fluorescence microscope. The hydrogels in water above the LCST were nontransparent and became transparent a few seconds after being taken out of the water. When the PNIPAM chains stays at the globule state, the phase separated morphologies of hydrogels were recorded.

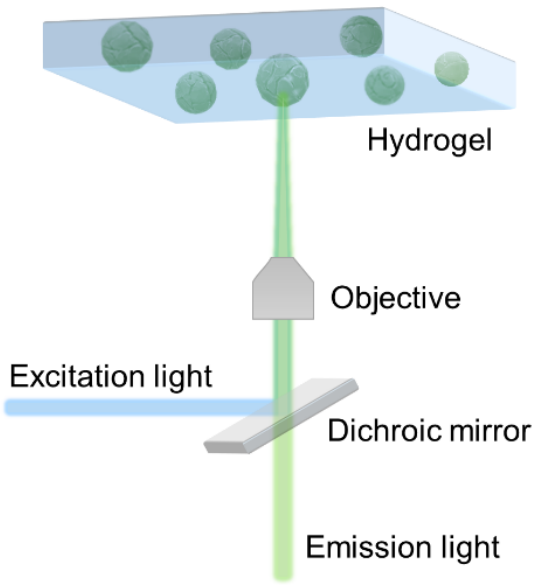


**Figure S14**. The observations of fluorescent composite hydrogels and the light path through an inverted fluorescence microscope.

**Light interference**

To better explain the optics phenomenon in the fluorescent images, we draw the following schematic diagram to illustrate the light interference in the microphase separation of composite hydrogels. The difference in refractive index of PNIPAM-rich phase and PDMA-rich phase induce the distinct regions in the fluorescent images, indicating the direct observation of phase separation morphologies.

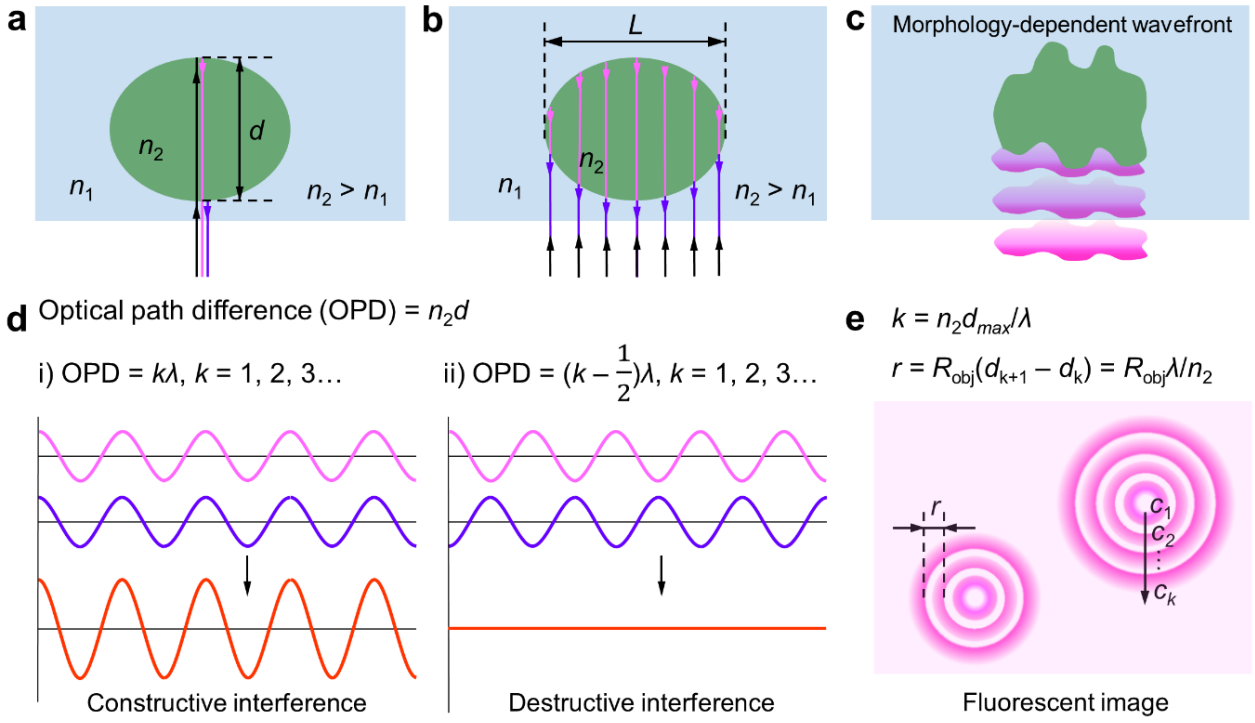


**Figure S15**. The proposed schematic illustration of light interference in the fluorescent composite hydrogels. (**a**) The excitation light (black lines) enters the hydrogel matrix and spherical domains with different refractive index (*n*). The emission light from both side of spherical domains (pink and purple lines) can induce light interference when the distance (*d*) is comparable to the wavelength of emission light. (**b**) The interference pattern varies due to the changing distance of spherical domains along the length (*L*) direction. (**c**) The morphology of polymer domains can be reflected by the interference patterns. (**d**) The constructive interference occurs when the optical path difference (OPD) equals to an integer multiple (*k*) of the light wavelength ($\lambda$). The destructive interference occurs when OPD equals the (k – 1/2) times of $\lambda$. (**e**) In the obtained fluorescent images, the numbers of interference fringes ($C_k$) in Newton's rings is correlated with the largest

distances of polymer domains. The fringe spacing ($r$) depends on the refractive index and the influence factor ($R_{obj}$) brought by the objectives in fluorescence microscope.

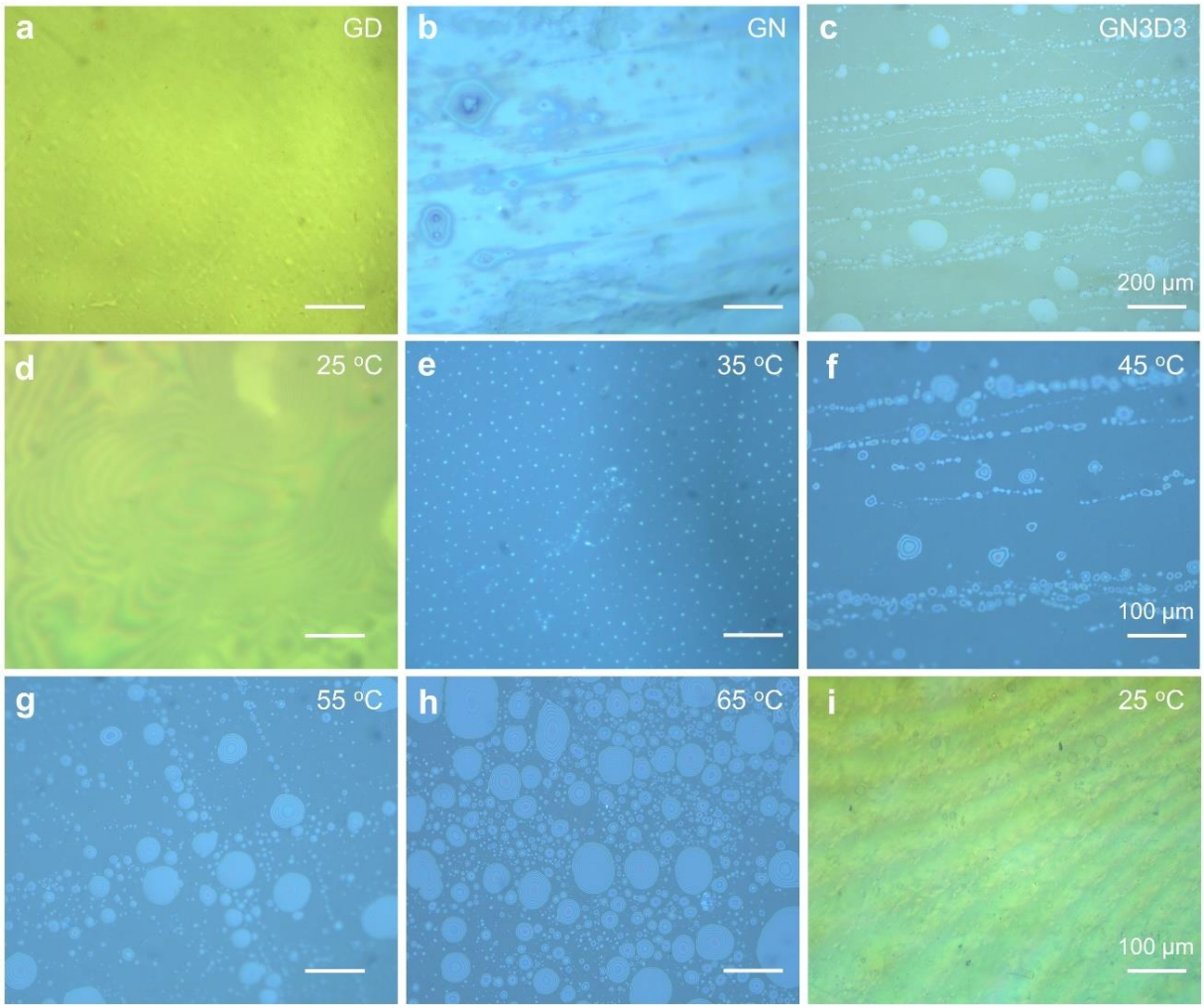


**Figure S16**. **a–c**, Fluorescent images of (**a**) GD, (**b**) GN, and (**c**) GN3D3 after immersing in water at 60 °C. **d–i**, Fluorescent images of GN3D3 immersing in water at (d) 25 °C, (e) 35 °C, (f) 45 °C, (g) 55 °C, (h) 65 °C and (i) after 5 h recovery at 25 °C.

**Rheology**

The viscoelastic properties of the hydrogels at the preparation state were studied. All the experiments were performed in the linear viscoelastic regime at 0.1% strain amplitude. All the hydrogel samples were immersed in paraffin oil during experiments to avoid drying. The GN2D3 samples were heated in oil at 60 °C for 30 min to avoid the volume change during the temperature-

dependent experiment. Frequency sweeps were performed with angular frequency from 1 to 100 rad/s. Temperature sweeps were performed at 1 rad/s and dynamic moduli (*G'* and *G''*) were recorded between 20 and 60 °C by applying a heating and cooling scan at a rate of 0.25 °C/min.

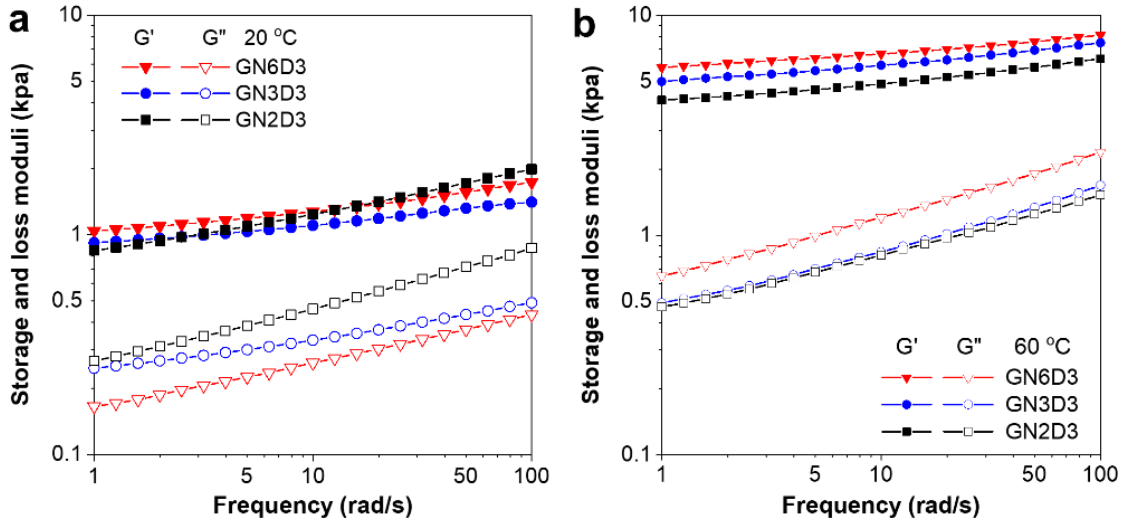


**Figure S17**. Frequency dependent storage (solid symbols, G') and loss (open symbols, G") modulus of GN2D3, GN3D3 and GN6D3 at (**a**) 20 °C and at (**b**) 60 °C.

**Tensile tests for large strain behavior**

The hydrogel samples were cut with a punch and their dimensions were 30 mm x 5 mm x 2 mm. The gauge length was recorded before each tensile experiment. For high temperature experiment, the hydrogel samples were immersed in paraffin oil bath and stabilized at designated temperature for 20 min. The GN2D3 samples were heated at 60 °C in oil for 20 min and their final dimensions were collected as 26 mm x 4.5 mm x 1.6 mm. All the tests were carried out at the same strain rate of 0.06 $s^{-1}$. Nominal stress was defined as $\sigma = F/S_0$, with $F$ being the recorded force and $S_0$ being the initial cross section. Reduced stress ($\sigma_R$) was calculated by the following equation of $\sigma_R = \sigma/(\lambda - \lambda^{-2})$, with σ being the nominal stress and $\lambda$ being the elongation calculated by $\lambda = L/L_0 = 1 + \sigma$.

**Fracture tests of pre-cracked hydrogels**

Fracture tests were performed using the single edge notch geometry on a standard tensile Instron machine model 5565 equipped with a 10 N load cell. A notch of approximately 1 mm length was made on the edge of hydrogel strips. The fracture energy ($G_c$) has been calculated by the

following equation[5]: $G_c = (6 \cdot W \cdot c)/\sqrt{\lambda_c}$ with $c$ being the initial notch length, $\lambda_c$ being the fracture strain and $W$ being the strain energy density calculated by integration of the stress-strain curve.

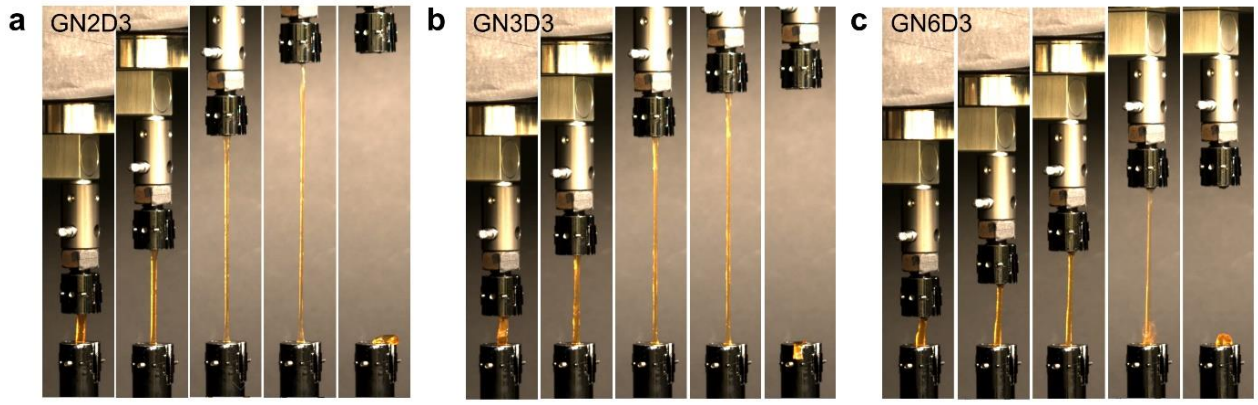


**Figure S18**. Tensile tests of GN2D3, GN3D3 and GN6D3 at 20 °C.

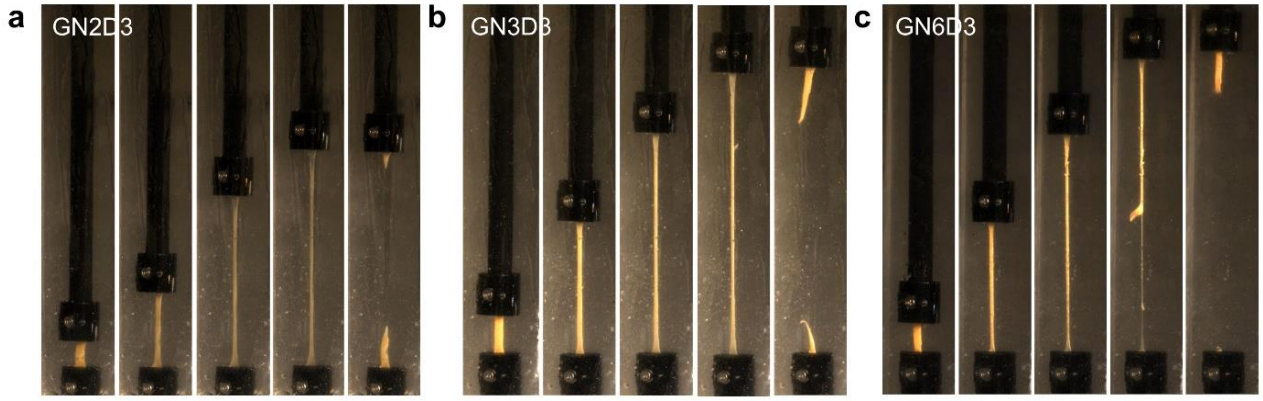


**Figure S19.** Tensile tests of GN2D3, GN3D3 and GN6D3 in paraffin oil baths at 60 °C.

**Temperature-dependent infrared spectroscopy**

Temperature-dependent infrared spectroscopy measurements of the GN hydrogel were conducted upon heating process from 25 to 60 °C. The absorption bands at 1628, 1560 and 1530 $cm^{-1}$ can be attributed to the C=O hydrogen bonded with H-O-H, the N-H hydrogen bonded with O-H2, and the N-H hydrogen bonded with O=C, respectively.[6] The gradual decrease in peak intensity at around 1628 $cm^{-1}$ and the continuous shift of peak frequencies from 1560 to 1530 $cm^{-1}$ can be clearly

observed. This indicates that C=O and N-H groups dehydrate above the LCST, while new hydrogen bonds between N-H and O=C of neighboring amide groups are formed.

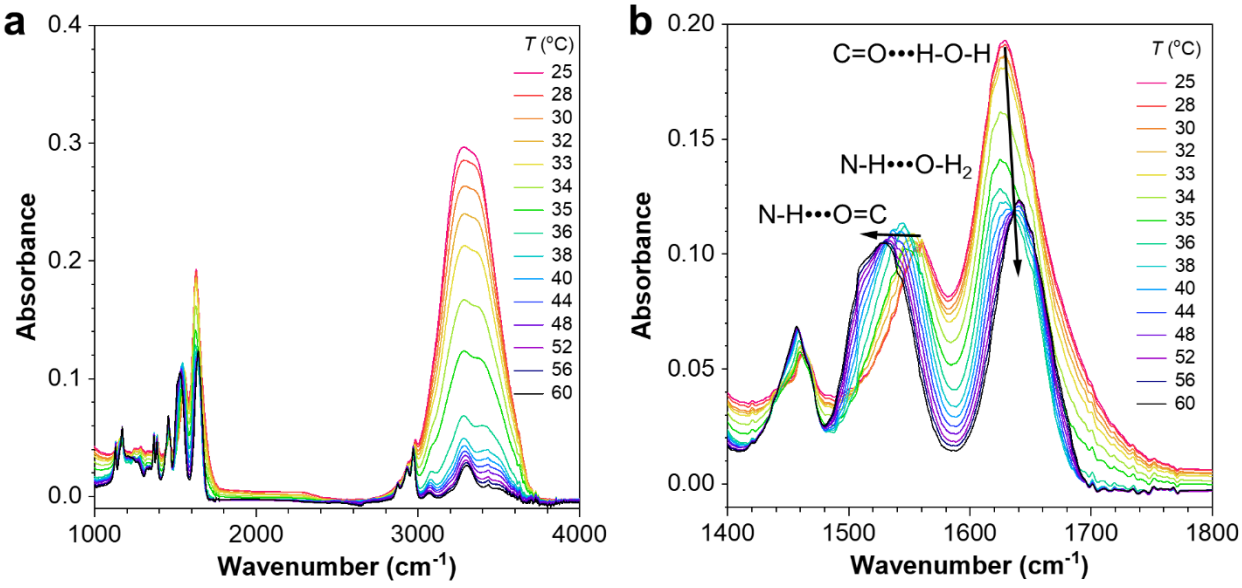


**Figure S20**. (**a**) Temperature-dependent infrared spectra of the GN hydrogel over the frequency range from 1000 to 4000 $cm^{-1}$. (**b**) Temperature-dependent infrared spectra of GN hydrogel over the frequency range from 1400 to 1800 $cm^{-1}$. The inset arrows represent the shift of peak frequencies upon heating process from 25 to 60 °C.

## References


(1) Barlow, T. R.; Brendel, J. C.; Perrier, S. Poly (bromoethyl acrylate): A reactive precursor for the synthesis of functional RAFT materials. *Macromolecules* **2016,** *49*, 6203-6212.

(2) Yang, Y.; Wang, X.; Yang, F.; Shen, H.; Wu, D. A universal soaking strategy to convert composite hydrogels into extremely tough and rapidly recoverable double-network hydrogels. *Adv. Mater*. **2016,** *28*, 7178-7184.

(3) Li, J.; Harada, A.; Kamachi, M. Sol–gel transition during inclusion complex formation between α-cyclodextrin and high molecular weight poly (ethylene glycol) s in aqueous solution. *Polym. J.* **1994,** *26*, 1019-1026.

(4) Lee, S. Y.; Lee, Y.; Kim, J. E.; Park, T. G.; Ahn, C.-H. A novel pH-sensitive PEG-PPG-PEG copolymer displaying a closed-loop sol–gel–sol transition. *J. Mater. Chem.* **2009,** *19*, 8198-8201.

(5) Greensmith, H. Rupture of rubber. X. The change in stored energy on making a small cut in a test piece held in simple extension. *J. Appl. Polym. Sci.* **1963,** *7*, 993-1002.

(6) Futscher, M. H.; Philipp, M.; Müller-Buschbaum, P.; Schulte, A. The role of backbone hydration of poly (N-isopropyl acrylamide) across the volume phase transition compared to its monomer. *Sci. Rep.* **2017,** *7*, 1-10.